Check for updates

Bulk phase behavior of lithium imide–metal nitride ammonia decomposition catalysts†‡

Joshua W. Makepeace, [ID] *[ab] Thomas J. Wood, [ID] [b] Phillip L. Marks, [ab] Ronald I. Smith, [b] Claire A. Murray [ID] [c] and William I. F. David *[ab]

Lithium imide is a promising new catalyst for the production of hydrogen from ammonia. Its catalytic activity has been reported to be significantly enhanced through its use as a composite with various transition metal nitrides. In this work, two of these composite catalysts (with manganese nitride and iron nitride) were examined using *in situ* neutron and X-ray powder diffraction experiments in order to explore the bulk phases present during ammonia decomposition. Under such conditions, the iron composite was found to be a mixture of lithium imide and iron metal, while the manganese composite contained lithium imide and manganese nitride at low temperatures, and a mixture of lithium imide and two ternary lithium–manganese nitrides ($Li_xMn_{2−x}N$ and a small proportion of Li_7MnN_4) at higher temperatures. The results indicate that the bulk formation of a ternary nitride is not necessary for ammonia decomposition in lithium imide–transition metal catalyst systems.
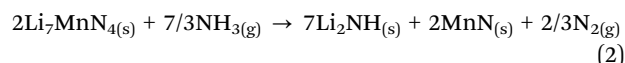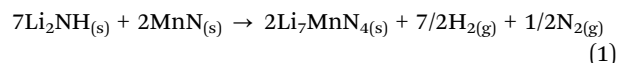
Introduction

In addition to being the feedstock for fertilisers that produce roughly half the global food supply,[1] ammonia has significant potential for use as a sustainable fuel. The combination of its relatively high volumetric energy density and clean combustion emission profile makes ammonia an attractive energy storage choice for transportation and inter-seasonal grid balancing applications. In order to facilitate its use in low-temperature fuel cells, or to promote its combustion,[2] ammonia must be either partially or completely cracked into hydrogen and nitrogen. Therefore, the development of highly active catalysts for the decomposition of ammonia is key to its successful application as a fuel.[3]

Catalysts for ammonia cracking have predominantly consisted of transition metal nanoparticles supported on porous carbon or oxide supports. Ruthenium is widely accepted to be the most active transition metal for this reaction, and so research efforts have focussed on the optimisation of ruthenium-based catalysts[4] (although iron and nickel catalysts are still of relevance as their low cost allows for higher metal loadings to compensate for their lower intrinsic activity[5]).

Since initial reports on the promising performance of sodium amide ($NaNH_2$) as an alternative catalyst to traditional transition metal systems,[6] lithium amide–imide ($LiNH_2–Li_2NH$) has emerged as the most important metal amide/imide ammonia decomposition catalyst, having shown high activity on its own[7] and as part of a mixed metal imide.[8] In both these cases the reported high-temperature ammonia decomposition activity was superior to supported ruthenium and nickel catalysts.

Very high catalytic activity can also be obtained by creating intimate mixtures of lithium imide with transition metals/ metal nitrides,[9–11] with lithium imide–manganese nitride mixtures showing superior activity (of around 27 kg_{NH_3} $kg_{cat}^{−1}$ $h^{−1}$) to a 5 wt% ruthenium on carbon nanotube catalyst, which is one of the most active ammonia decomposition catalyst formulations. These composites are proposed to function by the cyclical formation and decomposition of ternary nitrides. With manganese nitride, for example, the proposed reactions are as follows:

$$7Li_2NH_{(s)} + 2MnN_{(s)} \rightarrow 2Li_7MnN_{4(s)} + 7/2H_{2(g)} + 1/2N_{2(g)} \quad (1)$$

$$2Li_7MnN_{4(s)} + 7/3NH_{3(g)} \rightarrow 7Li_2NH_{(s)} + 2MnN_{(s)} + 2/3N_{2(g)} \quad (2)$$

The net reaction for the sum of reactions (1) and (2) is the decomposition of ammonia into nitrogen and hydrogen, eqn (3):

$$NH_{3(g)} \rightarrow 1/2N_{2(g)} + 3/2H_{2(g)} \quad (3)$$
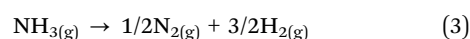
[a] *Inorganic Chemistry Laboratory, University of Oxford, South Parks Road, Oxford, OX1 3QR, UK. E-mail: josh.makepeace@chem.ox.ac.uk, bill.david@stfc.ac.uk*

[b] *ISIS Pulsed Neutron and Muon Facility, Rutherford Appleton Laboratory, Harwell Campus, Didcot, OX11 0QX, UK*

[c] *Diamond Light Source, Rutherford Appleton Laboratory, Harwell Campus, Didcot, OX11 0DE, UK*

† The research materials supporting this publication can be accessed by contacting Joshua Makepeace. Neutron diffraction data included in this publication will be publicly available at https://data.isis.stfc.ac.uk/ from 23/2/2019.

‡ Electronic supplementary information (ESI) available. See DOI: 10.1039/c8cp02824a

This journal is © the Owner Societies 2018

Phys. Chem. Chem. Phys., 2018, **20**, 22689–22697 | 22689

While each of these reactions has been demonstrated in isolation, the active form of these catalysts has yet to be identified. A recent isotopic study of the decomposition of ammonia by lithium imide indicated that a lithium-rich species may be a likely intermediate in the reaction, but it was concluded that this was unlikely to be a ternary nitride.[12] In this study, we use *in situ* neutron powder diffraction to probe the identity and structural character of two of the most active of these composite catalysts: lithium–imide/manganese nitride and lithium–imide/iron nitride. These experiments represent a characterisation of the bulk behaviour of these catalyst composites, which is of elevated significance in metal amide/imide systems due to the demonstrated bulk interaction of these catalysts with ammonia,[7,8,12,13] rather than a surface-confined reaction. However, it should be clear to the reader that the surface and interface behaviour of the materials is not the subject of this work.

Experimental

Synthesis

All sample manipulations were performed in an argon-filled glove box due to the air and moisture sensitivity of the materials (O_2, H_2O < 0.1 ppm). Deuterated lithium amide ($LiND_2$, 99% by XRD: ESI,‡ Fig. S1) was prepared by the reaction of lithium nitride (Li_3N, 98%, Sigma Aldrich) with 3 bar of deuterated ammonia (ND_3, 99%, 99 atom% D, Aldrich) at 300 °C for 3 hours. The powdered nitride was sealed in a cylindrical stainless steel reactor (I.D. 16 mm, height 100 mm) and attached to a gas panel. The reactor was evacuated and refilled with ammonia, and heated at 2 °C min^{-1} to the desired temperature. After reaction, the reactor was again evacuated, with the product powder extracted in the glove box. The lithium amide product was then hand-ground with one molar equivalent of lithium nitride for 15 minutes and heated in the same reactor under 1 bar of static argon pressure at 2 °C min^{-1} to 250 °C and held at that temperature for 12 hours to form deuterated lithium imide (Li_2ND). The purity of the synthesised material was determined to be greater than 95% (with minor impurities of lithium oxide and lithium nitride) by powder X-ray diffraction (see ESI,‡ Fig. S2).

Iron nitride ($Fe_{2-4}N$, Alfa Aesar) was used as received. Analysis of the XRD pattern (see ESI,‡ Fig. S3) of the material gave an average iron stoichiometry of $Fe_{3.5}N$ from a mixture of Fe_3N and Fe_4N. Manganese nitride (MnN) was synthesised by the reaction of manganese powder (Mn, 99.95%, Alfa Aesar) with 60 cm^3 min^{-1} flowing ammonia at 1 bar and 480 °C for 60 hours. The powder was placed inside a cylindrical stainless steel reactor (diameter 24.1 mm, height 100 mm) fitted with a gas inlet pipe running from the reactor lid to 10 mm from the base of the reactor. The gas outlet was located in the lid of the reactor, enabling gas flow over the top of the powder. The reactor was heated in a tube furnace (Severn Thermal Solutions) to the required temperature at 5 °C min^{-1}. Analysis of the XRD pattern of the product indicated that the sample was 91 wt% MnN and 9 wt% MnO (see ESI,‡ Fig. S4).

The mixed lithium-imide/metal-nitride samples were prepared by mixing the deuterated lithium imide with the appropriate metal nitride in a 1:1 molar ratio (the average stoichiometry of the iron nitride sample was used for this calculation). The mixtures were ground by hand for approximately 20 minutes to ensure an intimate mixture of the two reactants. These mixtures were then placed in a tungsten carbide milling jar filled with nine, 10 mm-diameter tungsten-carbide balls, sealed and milled in a planetary ball mill (PM100, Retszch) for 5 hours at 400 rpm, broken up into 15 minute segments. After each segment, the milling was paused for two minutes and the direction of rotation of the mill was reversed. This method was chosen in preference to the reaction of the metal chloride with lithium amide[9–11] as it eliminates the need to wash the deuterated samples with deuterated solvent in order to remove the lithium chloride by-product.

Powder diffraction

Time-of-flight neutron powder diffraction data of the two samples were collected using the POLARIS diffractometer[14] at the ISIS Pulsed Neutron and Muon Facility, United Kingdom. The experimental setup for these experiments was very similar to that described in previous reports,[7,8] with a detailed description given in the ESI.‡ Briefly, the powder sample was loaded into a custom-designed stainless steel 'flow over' cell, which itself was housed within a furnace mounted into the diffractometer. Although steel itself can decompose ammonia, quartz reactors are unsuitable given the strong basicity of the lithium imide material, having been shown to react with SiO_2 under ammonia to form lithium silicates.[15] Previous tests of blank reaction cells have shown that the catalytic performance is significantly lower than with the added catalyst,[3] reaching only 39% conversion at 550 °C with a 10 sccm (standard cubic centimetres per minute) flow of ammonia. This is a necessary compromise in order to avoid unwanted reaction of the catalyst. After leak-checking, gas was flowed through the cell (5–15 sccm) using a custom gas panel, and then analysed by mass spectrometry. Neutron powder diffraction data were collected in 100 s segments throughout the experiment. Additional reference diffraction patterns were collected at room temperature from each of the two starting materials, held in vanadium cans (6 mm diameter).

The *in situ* neutron powder diffraction experiment was similar for each of the two samples. Firstly, the sample was heated to 550 °C under flowing argon. Heating under inert gas prior to exposure to ammonia minimises the formation of lithium amide, which will cause melting of the sample in the temperature range ~370–500 °C with potential blockage of the reaction cell. After equilibrating under argon, the gas flowing over the sample was switched to deuterated ammonia to examine the structure and composition of the samples while decomposing ammonia. The samples were equilibrated under a number of different ammonia flow/temperature regimes in order to explore potential variation in the active form of the catalyst. Finally, the gas flow was switched to natural isotopic abundance ammonia to perform a hydrogen–deuterium isotope exchange experiment.

22690 | *Phys. Chem. Chem. Phys.*, 2018, **20**, 22689–22697

This journal is © the Owner Societies 2018

A second *in situ* powder diffraction experiment was performed using X-rays at the Diamond Light Source, United Kingdom. A sample of $Li_2NH + MnN$ ($\sim$10 mg) was placed into a 1 mm diameter sapphire capillary, held in place by a plug of quartz wool (out of the hot zone to avoid reaction with the catalyst), and was loaded into a custom gas flow cell.[16] The cell was leak checked and mounted on the I11 beamline.[17] It was placed under a 1 sccm flow of helium gas and heated to 500 °C using a hot air blower before the gas was switched to ammonia (1 sccm). After equilibrating, the ammonia flow rate was increased to 2 sccm in order to examine the effect of variable flow rate. This was followed by a switch back to helium, cooling of the sample to 475 °C, and a second exposure to ammonia (1 sccm) at this lower temperature. Diffraction data were collected in two-minute segments throughout the experiment, recorded using the high-resolution MAC detectors and an X-ray wavelength of 0.826209 Å.

The powder diffraction data were analysed using the TOPAS Academic[18] software package. A significant proportion of this analysis was performed using the batch analysis feature, where an initial refinement is performed, with the output then automatically used as the input for the refinement of the next dataset, and so on for all of the datasets. This allows for a large number of datasets with minor differences between them to be processed more efficiently.

Results and discussion

$Li_2ND + Fe_xN$

The results of the neutron powder diffraction experiment for the Li_2ND/Fe_xN composite sample are shown in Fig. 1. During the initial heating under argon flow, a large release of N_2 and a smaller release of D_2 were recorded, beginning at around 380 °C. The diffraction data indicate that this event correlates with the sequential denitriding of the $Fe_{3-x}N$ (through a range of nitrogen content as evidenced by the smooth change in the lattice parameter during denitriding) and Fe_4N phases to form Fe metal (the intense peak at 2.05 Å), according to reactions 4 and 5:

$$Fe_3N_{(s)} \rightarrow 3Fe_{(s)} + 1/2N_{2(g)} \tag{4}$$

$$Fe_4N_{(s)} \rightarrow 4Fe_{(s)} + 1/2N_{2(g)} \tag{5}$$
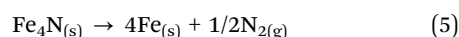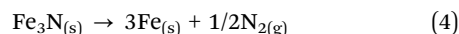
These reactions explain the release of nitrogen. The temperature of denitriding of $Fe_{3-x}N$ is broadly consistent with previous thermogravimetric analysis of the decomposition of iron nitrides.[19] The temperature of decomposition of Fe_4N is lower than that previously reported, which may relate to the presence of lithium imide, although significant thermal history effects were observed on the decomposition pathway of these materials.[19] The release of D_2 is consistent with the formation of the ternary
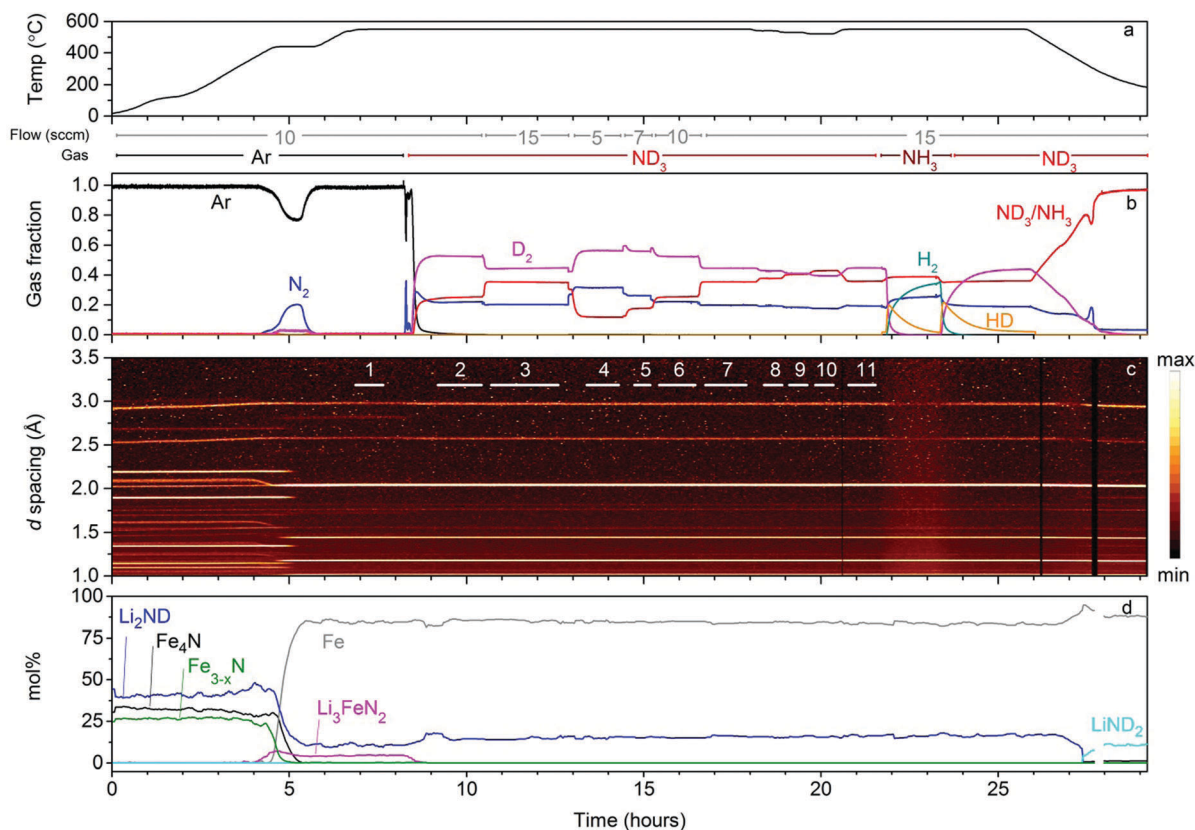

Fig. 1 Results of the neutron powder diffraction experiment on lithium imide–iron nitride. The panels show: (a) the temperature of the sample and gas flow rate and composition, (b) the molar gas fractions of the various gas species monitored in the experiment, (c) a contour plot of the neutron powder diffraction with regions used for analysis of summed diffraction data indicated with numbered, white lines and (d) a plot of the molar composition of the sample obtained from Rietveld analysis of the diffraction data.

This journal is © the Owner Societies 2018

Phys. Chem. Chem. Phys., 2018, **20**, 22689–22697 | **22691**

lithium–iron nitride, Li_3FeN_2, whose crystal structure appears in the powder diffraction data as the $Fe_{3-x}N/Fe_4N$ phases disappear:

$$3Li_2ND_{(s)} + Fe_4N_{(s)} \rightarrow 2Li_3FeN_{2(s)} + 2Fe_{(s)} + 3/2D_{2(g)} \qquad (6)$$
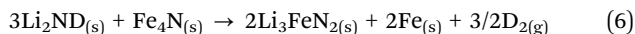
This is consistent with the results presented by Guo *et al.* for the reaction of Li_2NH and Fe_2N under inert gas.[9] The more nitrogen–poor nitrides used here (principally Fe_4N) result in the formation of Fe metal as well as the ternary nitride; the reaction did not go to completion, as Li_2ND remains present in the diffraction data and N_2 was the dominant gas species emitted from the sample. Thus, upon equilibration at 550 °C under argon, the sample consisted of a mixture of Fe, Li_2ND and Li_3FeN_2. Exposure of the sample to ND_3 at ~ 8.3 h resulted in a sharp emission of N_2 prior to the observation of any ND_3 in the outflow gas. The Bragg peaks associated with the Li_3FeN_2 phase disappeared rapidly, with a concomitant increase in the peak intensity for the Li_2ND phase. These observations are consistent with the ammoniation of Li_3FeN_2 according to reaction (7).

$$2Li_3FeN_{2(s)} + ND_{3(g)} \rightarrow 3Li_2ND_{(s)} + 2Fe_{(s)} + N_{2(g)} \qquad (7)$$
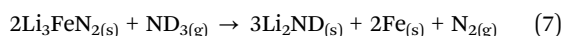
The high temperature of exposure of Li_3FeN_2 to ammonia explains why Fe is observed rather than iron nitride species reported in previous investigations of this reaction,[9,20] as the enhanced ammonia decomposition leads to a lower partial pressure of ammonia and higher hydrogen partial pressure, reducing the stability of the iron nitrides.[21] It is worth noting that the formation of iron nitrides might be expected from the ammonia gas fraction range in this experiment considering existing literature on the Fe–N phase diagram at varying nitrogen potentials.[22] However, the ammonia partial pressure in the catalyst bed is likely to be very low given the documented catalytic activity of lithium imide catalysts,[7,9] with the higher ammonia gas fraction likely due to ammonia which does not interact with the catalyst bed as a result of the flow-over sample geometry.

Examination of the remainder of the diffraction data shows that, aside from small variations in stoichiometry which will be discussed in the following text, the sample remains as a mixture of Li_2ND and Fe throughout the range of ammonia decomposition reaction conditions explored. Only once the reaction is cooled under ND_3 can the reformation of a small amount of Fe_4N be observed together with release of D_2 (at approximately 27.5 h), along with the conversion of Li_2ND to $LiND_2$ through a melt. This suggests that if the ammonia decomposition mechanism in this system relies on the formation of the ternary nitride, then it must only exist as a short-lived intermediate. Given the large particle sizes indicated by the sharp Bragg peaks observed for the crystalline phases, it seems unlikely that the bulk of the sample is being rapidly converted between the ternary nitride and the Li_2ND–Fe composite. Thus, if the ternary nitride is indeed the active species, the ammonia decomposition reaction must only take place on the interface of Li_2ND and Fe particles. The ammonia fraction observed for this sample at 550 °C and 10 sccm ND_3 flow is approximately the same as was observed for Li_2ND on its own in a similar experimental setup.[7]

After equilibrating under ND_3, the sample was then exposed to a number of different ND_3 flow rate and temperature regimes. Visual inspection of the diffraction data presented in Fig. 1c indicates that no significant changes in the phase composition of the sample were observed under the conditions used, despite the ammonia gas fraction clearly changing with changing conditions, *i.e.* a higher ammonia gas fraction at higher ND_3 flow rates and lower temperatures, as indicated in Fig. 1b.

A more detailed analysis of the sample was performed by Rietveld analysis of summed sections of the diffraction data where the ammonia gas fraction was stable for each flow/temperature regime (see ESI,‡ Fig. S6 for an illustration of the summed regions). Of particular interest are potential changes in the stoichiometry of Li_2ND towards $LiND_2$ (forming $Li_{1+x}ND_{2-x}$), which have previously been observed in the context of ammonia decomposition reactions.[7] Fig. 2 shows the refined lattice parameter and lithium occupancy of the Li_2ND phase from each summed diffraction dataset under the various reaction conditions of the experiment, with the lattice parameter of the Fe phase included as a reference (fits to each summed dataset are given in the ESI,‡ Fig. S7–S17).

Attempts to directly refine the stoichiometry of the sample using the summed diffraction data (see the lithium occupancy in Fig. 2) did not show any significant changes over the different segments; the analysis was hindered by the relatively poor signal-to-noise ratio in the peaks associated with the Li_2ND phase. However, the lattice parameter data provide a more robust measure of the subtle changes in the sample under the various reaction conditions. While the variation in the Fe lattice parameter is consistent with normal thermal expansion behaviour, the variation in Li_2ND lattice parameter is more complex.

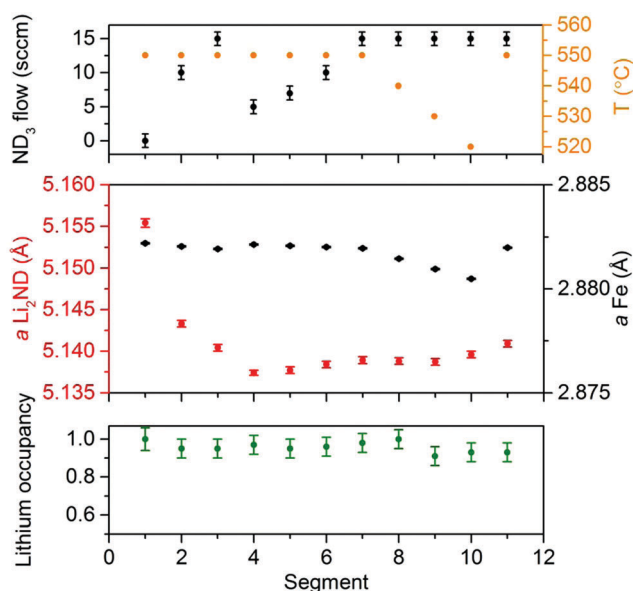Fig. 2 Refined lattice parameter and lithium occupancy for the $Li_{1+x}ND_{2-x}$ phase in the $Li_2ND + Fe_xN$ sample under the various temperature/ND_3 flow segments of the *in situ* neutron diffraction experiment. Error bars represent one standard deviation.

22692 | *Phys. Chem. Chem. Phys.*, 2018, **20**, 22689–22697

This journal is © the Owner Societies 2018

Changes in the lattice parameter of lithium imide have been associated with variation in the sample stoichiometry in previous ammonia decomposition[7] and hydrogen storage[23] *in situ* diffraction measurements. In general, these studies have shown that a larger lattice parameter is associated with a more hydrogen-rich phase (although a recent study on the room-temperature structure of a number of lithium amide–imide non-stoichiometric phases synthesised by reaction of lithium nitride with lithium amide showed the opposite trend[24]).

The Li_2ND lattice parameter decreased dramatically on initial exposure of the sample to ND_3 (segment $1 \rightarrow 2$), with a further decrease in segment 3 despite an increase in the ND_3 flow rate. Both of these segments would be expected to show in an increase in the lattice parameter associated with a shift toward amide stoichiometry, based on the previous results. This may indicate that the Li_2ND which remained after the formation of the ternary nitride has a different stoichiometry or defect structure than the Li_2ND formed by decomposition of the ternary nitride on exposure to ND_3. A plot of the variation in the lattice parameter of Li_2ND in each individual run throughout the experiment (ESI,‡ Fig. S18) shows that on exposure to ND_3, an initial exponential decrease in the lattice parameter is followed by a much slower decrease (fit here with a linear function). This process appears to not have completed before the flow was changed in segment 3. Therefore, the lattice parameter continues to decrease, though at a slower rate, which may be as a result of the higher ammonia flow rate.

Segments 4–7 are an isothermal region where the ND_3 flow rate was sequentially increased between 5 sccm and 15 sccm. The lattice parameter increases with the increasing flow, which is consistent with increasing hydrogen (deuterium) content through absorption of ammonia:

$$(1 + x)Li_2ND_{(s)} + (1-x)ND_{3(g)} \rightarrow 2Li_{1+x}ND_{2-x(s)} \quad (8)$$
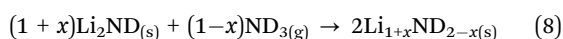
In segments 7–10 in Fig. 2, the ND_3 flow rate was held constant while the temperature was decreased in 10 °C steps. In this case, the change in stoichiometry is more difficult to observe, as lowering the temperature causes contraction of the sample, while simultaneously favouring reaction (8), which is seen to increase the lattice parameter. The net effect is no significant change in the lattice parameter when the temperature was lowered to 540 °C and 530 °C, followed by a slight increase when lowered to 520 °C.

In order to probe these data, the thermal expansion of the Li_2ND lattice during the heating under argon was calculated. The 150–400 °C section was used, as the heating ramp rate was almost constant in that range. The thermal expansion coefficient from the linear fit of these data (ESI,‡ Fig. S19) was then used to predict the expected change of the Li_2ND lattice parameter with the temperature changes in segments 7–10. These predicted values are compared with the measured values in Fig. 3, showing the measured lattice parameter is significantly larger than expected from the thermal expansion data, again reflecting absorption of ammonia. Comparison of these with the lattice parameters for increasing ND_3 flow
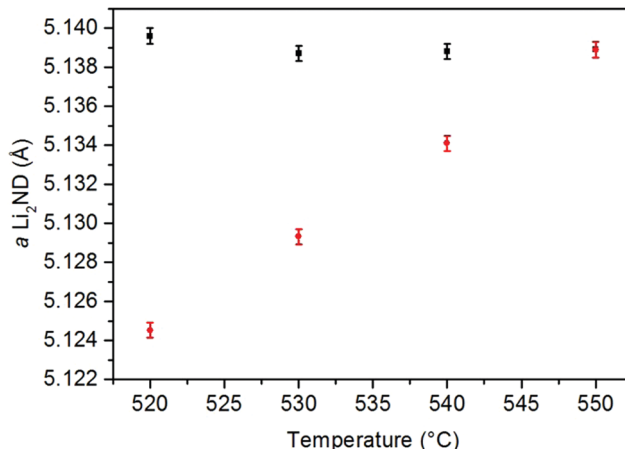

Fig. 3 Comparison of the lattice parameter of Li_2ND at various temperatures extracted from the Rietveld analysis of the measured diffraction data (black squares) with the value predicted from the thermal expansion coefficient (red circles). Error bars represent one standard deviation.

highlights the strong influence of temperature on the stoichiometry of lithium imide under ammonia.

The increase in temperature back to 550 °C in segment 11 results in a larger lattice parameter than was observed under the same conditions in segment 7. This is due to the slow kinetics of the reverse reaction of reaction (8).

The final stage of the experiment, beginning at 21.8 h, was a hydrogen–deuterium isotope exchange experiment where natural abundance ammonia gas was introduced in place of ND_3. In the section of the diffraction data following this change, the background intensity can be seen to increase, along with a significant decrease in the intensity (and relative intensities) of the Bragg peaks of the Li_2ND phase. The intensities of the Fe peaks were unaffected. This is as a result of the incoherent neutron scattering of hydrogen as it is incorporated into the lithium imide structure. Rietveld analysis of the diffraction data in this section shows the structure changing from completely deuterated to completely hydrogenated, with a concomitant decrease in the lattice parameter (ESI,‡ Fig. S20). Reintroduction of ND_3 shows the exchange to be reversible.
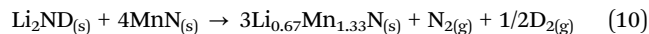
Under ammonia, this sample showed similar behaviour to that observed for lithium imide in isolation in the previous *in situ* study, with the addition of the iron phase. While the formation of the ternary imide Li_3FeN_2 was observed under inert gas, no ternary phases were observed under ND_3 in this measurement of bulk structure. This may indicate a very short lifetime for this intermediate or that the formation of the ternary phase is confined to the surface, which cannot be effectively measured in this experiment.

Li_2ND + MnN

The results of the neutron diffraction experiment on the lithium imide–manganese nitride composite are summarised in Fig. 4. The experiment proceeded similarly to the iron composite sample. During heating under argon, two distinct gas release events were observed with peaks at 483 °C and 550 °C. The higher relative

amount of D_2 in the gas release events compared with the iron sample reflects more complete conversion of the sample to ternary lithium–manganese nitrides. Li_2ND was completely consumed and converted into two ternary nitrides: Li_7MnN_4 and $Li_xMn_{2-x}N$.

$$7Li_2ND_{(s)} + 2MnN_{(s)} \rightarrow 2Li_7MnN_{4(s)} + 7/2D_{2(g)} + 1/2N_{2(g)} \quad (9)$$

$$Li_2ND_{(s)} + 4MnN_{(s)} \rightarrow 3Li_{0.67}Mn_{1.33}N_{(s)} + N_{2(g)} + 1/2D_{2(g)} \quad (10)$$

The formation of Li_7MnN_4 was reported by Guo *et al.*, but $Li_xMn_{2-x}N$ was not observed. The phase was first synthesised by reaction of lithium nitride with manganese under a nitrogen atmosphere,[25] with disordered lithium and manganese occupancy of the cation sites in an anti-Rutile structure type. The authors of this study indicated that variable lithium occupancy was possible in the structure. An attempt to refine the lithium occupancy of the $Li_xMn_{2-x}N$ phase formed in this experiment resulted in zero lithium occupancy (*i.e.* Mn_2N). However, the structure is not one of the Mn_2N polymorphs. Furthermore, the authors of the study on $Li_xMn_{2-x}N$ state that below $x = 0.333$, only Mn_2N is formed.[25] While the full range of variable lithium content in the phase has not yet been characterised, we take the minimum value of x in $Li_xMn_{2-x}N$ to be 0.333 as a guide (hence the stoichiometry in reaction (10)).

The $Li_xMn_{2-x}N$ phase forms rapidly, while the kinetics of formation of the Li_7MnN_4 phase are relatively slow, with D_2 production observed until just before 10 h. At the end of the period under argon, these two phases account for all of the Bragg peaks in the diffraction data (excluding the steel from the reaction cell).

On introduction of ND_3, the Li_2ND peaks reappeared with the almost complete decomposition of the Li_7MnN_4, in a similar fashion to Li_3FeN_2, with a broader nitrogen release observed in the mass spectrometry data between 11.5 and 13 h:

$$6Li_7MnN_{4(s)} + 7ND_{3(g)} \rightarrow 21Li_2ND_{(s)} + 6Mn_{(s)} + 5N_{2(g)} \quad (11)$$
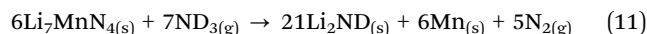
A small amount (~ 10–20 wt%) of Mn was formed during the decomposition and was identified in the Rietveld analysis. Recent neutron powder diffraction studies of the reaction of manganese under flowing ammonia detected the slow transformation of manganese to Mn_4N, Mn_2N and Mn_3N_2 in this temperature range.[26,27] The absence of any of these phases in this experiment is likely as a result of the higher hydrogen partial pressure and lower ammonia partial pressure due to the ammonia decomposition reaction, as described for the iron sample.

The relatively low intensity of the manganese metal Bragg peaks and their partial overlap with the $Li_xMn_{2-x}N$ phase made
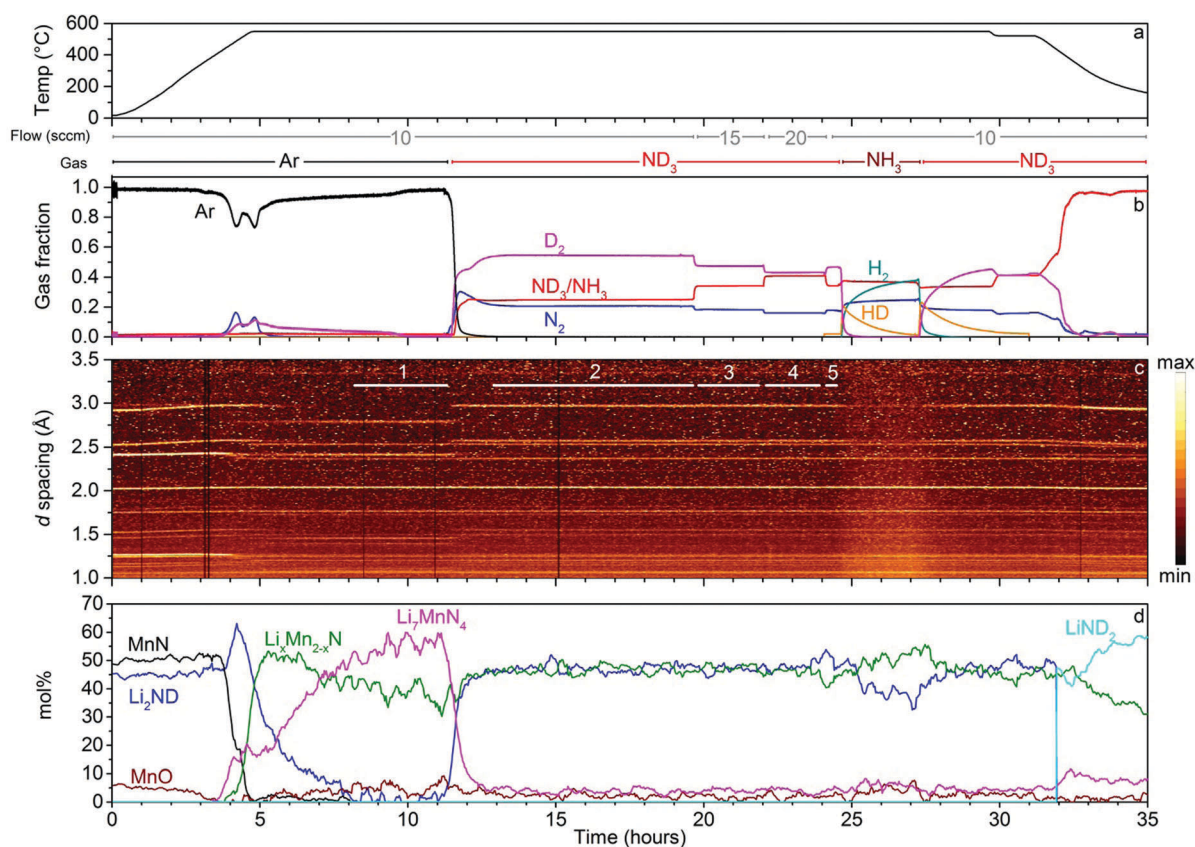

Fig. 4 Results of the neutron powder diffraction experiment on lithium imide–manganese nitride. The panels show (a) the temperature of the sample and gas flow rate and composition, (b) the molar gas fractions of the various gas species monitored in the experiment, (c) a contour plot of the neutron powder diffraction with regions used for analysis of summed diffraction data indicated with numbered, white lines and (d) the molar composition of the sample obtained from Rietveld analysis of the diffraction data.

22694 | *Phys. Chem. Chem. Phys.*, 2018, **20**, 22689–22697

This journal is © the Owner Societies 2018

the batch refinement unstable (ESI,‡ Fig. S21). As a result it was not included in the main analysis. Additionally, extra weak Bragg peaks associated with an unidentified phase(s) were observed in the summed data under ND_3. It is possible that these peaks are associated with either a nitride of manganese or another ternary lithium–manganese nitride. All known phases in these two categories were checked against the peaks, but no satisfactory fits were obtained. Given the poor signal-to-noise ratio on these peaks and their limited number, it was not possible to index them and their origin remains unknown.

Unlike the iron-based sample, the ternary nitride phases remained present for this sample under ammonia decomposition conditions. A small amount of Li_7MnN_4 (~ 5 mol%) persisted in the sample, while the scale factor for the $Li_xMn_{2-x}N$ phase remained almost unchanged upon introduction of ND_3. Under a reducing gas environment such as is generated in ammonia decomposition conditions, the lower formal (1–2+) oxidation state of manganese in this nitride may be more stable than the Mn^{5+} present in Li_7MnN_4, which may explain the relative stabilities of the two nitride phases.

As with the Li_2ND/Fe_xN sample, the ND_3 flow rate was varied in order to study the active form of the catalyst over a range of reaction conditions. Increasing the ND_3 flow rate to 15 sccm and then 20 sccm resulted in slightly lower ammonia decomposition levels as expected, and again resulted in little change to the observed diffraction patterns. Refinement of the Li_2ND phase in summed diffraction datasets for these regions (ESI,‡ Fig. S23–S28) produced similar results to the iron-containing sample; and while a significant difference in the lithium occupancy was not detected, the change in ND_3 flow rate did result in a slight increase in the lattice parameter associated with a shift toward amide stoichiometry (Fig. 5).

Refinement of the Li_2ND lattice parameter and deuterium occupancy during the H–D isotope exchange experiment also showed almost complete and completely-reversible conversion of Li_2ND to Li_2NH (ESI,‡ Fig. S29), again demonstrating the bulk interaction of lithium amide–imide with ammonia.

The presence of both Li_2ND and $Li_xMn_{2-x}N$ under ammonia decomposition conditions in this experiment raises the question of whether the formation of the ternary nitride $Li_xMn_{2-x}N$ is necessary for ammonia decomposition. Fig. 6 details the results of an *in situ* synchrotron X-ray powder diffraction experiment on the $Li_2NH + MnN$ system. This experiment was conducted at the lower temperature of 500 °C to avoid oxidation of the sample through reaction with the sapphire capillary. In this experiment, no Li–Mn–N phases were observed, under helium gas or ammonia. MnN was found to persist in the sample throughout the experiment, undergoing a tetragonal to cubic phase transition at 460 °C (this is a somewhat higher temperature than has been reported from DSC measurements,[28] which may indicate a temperature difference between the set point of the system and the actual temperature of the sample inside the capillary). When the gas flow was switched to ammonia, the cubic MnN phase was unchanged, while a step increase in the size of the Li_2NH lattice can be seen (Fig. 6c, 135 min), consistent with a shift towards amide stoichiometry as explained previously. The increase in the
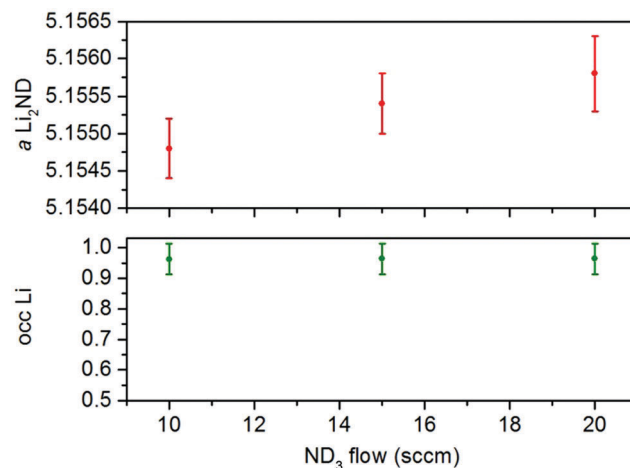

Fig. 5 Variation of the lattice parameter and lithium occupancy of the Li_2ND phase in the $Li_2ND + MnN$ composite under different ND_3 flow rates. Error bars represent one standard deviation.
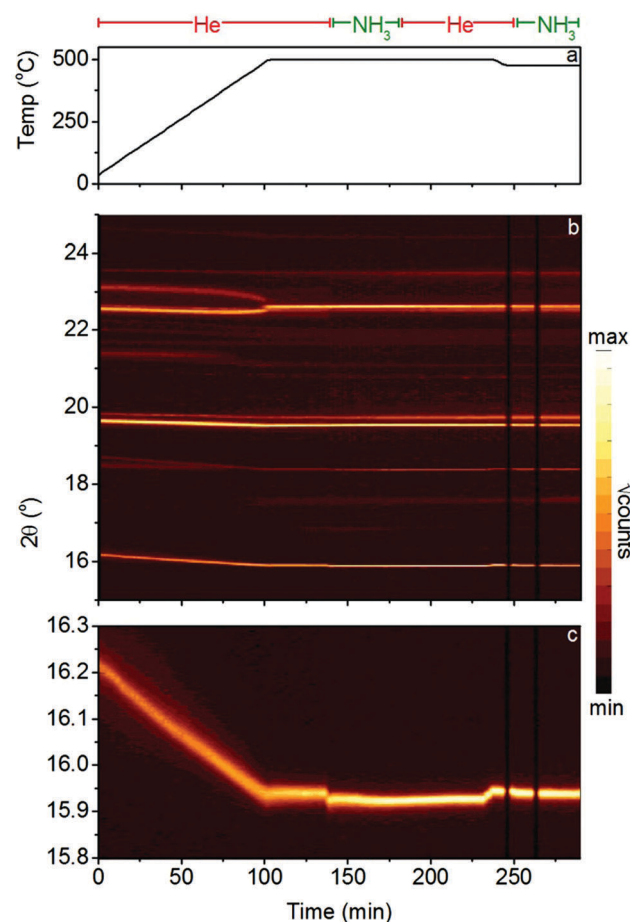

Fig. 6 *In situ* synchrotron X-ray diffraction on the ammonia decomposition reaction by the lithium imide–manganese nitride composite, showing (a) the gas species (1 sccm constant flow) and sample temperature, (b) contour plot of the diffraction data and (c) a contour plot of the $Li_2ND(111)$ region of the diffraction pattern.

ammonia flow rate from 1 sccm to 2 sccm (Fig. 6c, 150 min) shows a further, smaller increase in the lattice parameter,

This journal is © the Owner Societies 2018

Phys. Chem. Chem. Phys., 2018, **20**, 22689–22697 | 22695

indicating a further shift towards amide stoichiometry. The return to helium flow (Fig. 6c, 175 min) resulted in a gradual decrease in the Li_2NH lattice parameter, consistent with the return towards imide stoichiometry.

The absence of any Li–Mn–N phases in this experiment, while still in a temperature-flow regime where significant ammonia decomposition activity is expected,[10] suggests that the presence of such a phase in the bulk is not a prerequisite for ammonia decomposition. There was no evidence in the diffraction data for broad features which might be associated with nanoparticles or amorphous features, which suggests that the Rietveld analysis should accurately reflect the bulk phase composition of these samples. While this does not preclude the possibility that the ternary phase is present as a short-lived or surface/interface intermediate, as discussed previously, or that both Li_2ND and $Li_xMn_{2-x}N$ are active ammonia decomposition catalysts, it does suggest that these composites may be best described as promoted lithium imide catalysts.

Conclusions

Catalyst composites based on light metal amide and imide catalysts are promising low-cost systems for the generation of high-purity hydrogen from ammonia, showing improved performance over state-of-the-art ruthenium-based catalysts. *In situ* powder diffraction measurements of ammonia decomposition reactions catalysed by composites of lithium imide with manganese nitride and iron nitride have given insight into the active forms of these catalysts. While both systems were found to form ternary nitrides (Li_3FeN_2, $Li_xMn_{2-x}N$ and Li_7MnN_4) at elevated temperatures under inert gas, only $Li_xMn_{2-x}N$ was found to persist as a significant proportion of the sample under ammonia decomposition conditions. Li_3FeN_2 completely disappeared, while Li_7MnN_4 only remained as a minor component of the sample. Lithium imide was present under active conditions in both samples, and demonstrated stoichiometry variation consistent with previous reports on the structure of isolated lithium imide during ammonia decomposition. These results suggest that bulk formation of the ternary nitride is not a complete explanation of the reported enhancements in catalytic activity reported for these imide–nitride composites.

Conflicts of interest

There are no conflicts to declare.

Acknowledgements

References

1 J. W. Erisman, M. A. Sutton, J. Galloway, Z. Klimont and W. Winiwarter, How a Century of Ammonia Synthesis Changed the World, *Nat. Geosci.*, 2008, **1**, 636–639.

2 M. Comotti and S. Frigo, Hydrogen Generation System for Ammonia-Hydrogen Fuelled Internal Combustion Engines, *Int. J. Hydrogen Energy*, 2015, **40**, 10673–10686.

3 S. Mukherjee, S. V. Devaguptapu, A. Sviripa, C. R. F. Lund and G. Wu, Low-Temperature Ammonia Decomposition Catalysts for Hydrogen Generation, *Appl. Catal., B*, 2018, **226**, 162–181.

4 S. F. Yin, B. Q. Xu, X. P. Zhou and C. T. Au, A Mini-Review on Ammonia Decomposition Catalysts for on-Site Generation of Hydrogen for Fuel Cell Applications, *Appl. Catal., A*, 2004, **277**(1–2), 1–9.

5 F. Schüth, R. Palkovits, R. Schlögl and D. S. Su, Ammonia as a Possible Element in an Energy Infrastructure: Catalysts for Ammonia Decomposition, *Energy Environ. Sci.*, 2012, **5**(4), 6278.

6 W. I. F. David, J. W. Makepeace, S. K. Callear, H. M. A. Hunter, J. D. Taylor, T. J. Wood and M. O. Jones, Hydrogen Production from Ammonia Using Sodium Amide, *J. Am. Chem. Soc.*, 2014, **136**(38), 13082–13085.

7 J. W. Makepeace, T. J. Wood, H. M. A. Hunter, M. O. Jones and W. I. F. David, Ammonia Decomposition Catalysis Using Non-Stoichiometric Lithium Imide, *Chem. Sci.*, 2015, **6**, 3805–3815.

8 J. W. Makepeace, H. M. A. Hunter, T. J. Wood, R. I. Smith, C. A. Murray and W. I. F. David, Ammonia Decomposition Catalysis Using Lithium–Calcium Imide, *Faraday Discuss.*, 2016, **188**, 525–544.

9 J. Guo, P. Wang, G. Wu, A. Wu, D. Hu, Z. Xiong, J. Wang, P. Yu, F. Chang and Z. Chen, *et al.*, Lithium Imide Synergy with 3d Transition-Metal Nitrides Leading to Unprecedented Catalytic Activities for Ammonia Decomposition, *Angew. Chem., Int. Ed.*, 2015, **127**(10), 2993–2997.

10 J. Guo, F. Chang, P. Wang, D. Hu, P. Yu, G. Wu, Z. Xiong and P. Chen, Highly Active MnN–Li_2NH Composite Catalyst for Producing CO_x-Free Hydrogen, *ACS Catal.*, 2015, **5**(5), 2708–2713.

11 J. Guo, Z. Chen, A. Wu, F. Chang, P. Wang, D. Hu, G. Wu, Z. Xiong, P. Yu and P. Chen, Electronic Promoter or Reacting Species? The Role of $LiNH_2$ on Ru in Catalyzing NH_3 Decomposition, *Chem. Commun.*, 2015, **51**(82), 15161–15164.

12 T. J. Wood, J. W. Makepeace and W. I. F. David, Isotopic Studies of the Ammonia Decomposition Reaction Using Lithium Imide Catalyst, *Phys. Chem. Chem. Phys.*, 2017, **19**, 4719–4724.

13 T. J. Wood, J. W. Makepeace, H. M. A. Hunter, M. O. Jones and W. I. F. David, Isotopic Studies of the Ammonia Decomposition Reaction Mediated by Sodium Amide, *Phys. Chem. Chem. Phys.*, 2015, **17**(35), 22999–23006.

14 S. Hull, R. I. Smith, W. I. F. David, A. C. Hannon, J. Mayers and R. Cywinski, The Polaris Powder Diffractometer at ISIS, *Phys. B*, 1992, **181**, 1000–1002.

22696 | *Phys. Chem. Chem. Phys.*, 2018, **20**, 22689–22697

This journal is © the Owner Societies 2018

15 T. J. Wood and J. W. Makepeace, Assessing Potential Supports for Lithium Amide-Imide Ammonia Decomposition Catalysts, *ACS Appl. Energy Mater.*, 2018, **1**, 2657–2663.

16 J. E. Parker, J. Potter, S. P. Thompson, A. R. Lennie and C. C. Tang, *In Situ* Gas Supply System on the Powder Diffraction Beamline I11 at Diamond Light Source, *Mater. Sci. Forum*, 2012, **706–709**, 1707–1712.

17 S. P. Thompson, J. E. Parker, J. Potter, T. P. Hill, A. Birt, T. M. Cobb, F. Yuan and C. C. Tang, Beamline I11 at Diamond: A New Instrument for High Resolution Powder Diffraction, *Rev. Sci. Instrum.*, 2009, **80**(7), 075107.

18 A. Coelho, TOPAS-Academic, Version 6, http://www.topas-academic.net/.

19 M. Widenmeyer, T. C. Hansen, E. Meissner and R. Niewa, Formation and Decomposition of Iron Nitrides Observed by *In Situ* Powder Neutron Diffraction and Thermal Analysis, *Z. Anorg. Allg. Chem.*, 2014, **640**(7), 1265–1274.

20 W. Peikun, J. Guo and P. Chen, The Interactions of Li_3FeN_2 with H_2 and NH_3 Science Direct, *Int. J. Hydrogen Energy*, 2016, 1–7.

21 T. J. Wood, J. W. Makepeace and W. I. F. David, Neutron Diffraction and Gravimetric Study of the Iron Nitriding Reaction under Ammonia Decomposition Conditions, *Phys. Chem. Chem. Phys.*, 2017, **19**, 27859–27865.

22 B. J. Kooi, M. A. J. Somers and E. J. Mittemeijer, An Evaluation of the Fe-N Phase Diagram Considering Long-Range Order of N Atoms in Γ'-Fe_4N_{1-x} and ε-Fe_2N_{1-z}, *Metall. Mater. Trans. A*, 1996, **27**(4), 1063–1071.

23 J. W. Makepeace, M. O. Jones, S. K. Callear, P. P. Edwards and W. I. F. David, *In Situ* X-Ray Powder Diffraction Studies of Hydrogen Storage and Release in the Li–N–H System, *Phys. Chem. Chem. Phys.*, 2014, **16**, 4061–4070.

24 J. W. Makepeace and W. I. F. David, Structural Insights into the Lithium Amide–Imide Solid Solution, *J. Phys. Chem. C*, 2017, **121**, 12010–12017.

25 R. Niewa, F. DiSalvo, D.-K. Yang, D. Zax, H. Luo and W. Yelon, Synthesis, Crystal Structure and Properties of a Lithium Manganese Nitride, $(Li, Mn)_2N$, *J. Alloys Compd.*, 1998, **266**, 32–38.

26 M. Widenmeyer, T. C. Hansen, A. Leineweber, A. Weidenkaff and R. Niewa, Nitrogen Transfer between Solid Phases in the System Mn–N Detected *via in situ* Neutron Diffraction, *Z. Anorg. Allg. Chem.*, 2017, **643**(23), 1929–1938.

27 T. J. Wood, J. W. Makepeace and W. I. F. David, Neutron Diffraction and Gravimetric Study of the Manganese Nitriding Reaction under Ammonia Decomposition Conditions, *Phys. Chem. Chem. Phys.*, 2018, **20**, 8547–8553.

28 A. Leineweber, R. Niewa, H. Jacobs and W. Kockelmann, The Manganese Nitrides η-Mn_3N_2 and ΘMn_6N_{5+x}: Nuclear and Magnetic Structures, *J. Mater. Chem.*, 2000, **10**(12), 2827–2834.